



# Integrated Energy Multi-Agent Collaborative Optimization Regulation Method for Typhoon Events

Zhenlan Dou,<sup>1</sup> Chunyan Zhang,<sup>1</sup> Songcen Wang,<sup>3</sup> Yipan Zhang,<sup>4</sup> Tao Zhang<sup>5</sup> and Dejian Yang<sup>2,\*</sup>

## Abstract

Typhoon disasters pose severe challenges to the safe and stable operation of integrated energy systems. Traditional single energy regulation models are difficult to cope with the dynamic uncertainties in multi-energy flow coupled systems. In this study, a regulation method based on multi-agent collaborative optimization is proposed to achieve the dynamic balance of the electricity-gas-thermal multi-energy system under typhoon events by constructing a distributed decision-making framework. Experiments show that in the simulated line fault scenario caused by a typhoon, multi-agent cooperative regulation reduces the average voltage deviation of key nodes from 0.17 p.u. to 0.05 p.u., verifying the effect of the cooperative strategy on improving voltage stability. For the extreme scenario of a 24-hour continuous typhoon, this method improves the power supply reliability of the system from 82.3% to 95.6%, and the renewable energy consumption rate by 20.7 percentage points (from 68.5% to 89.2%). At the same time, through multi-energy complementation and demand-side response, comprehensive operating costs are reduced by 21.1%. Iterative analysis reveals that the five types of agents exhibit significant differentiation characteristics in the regulation process. Notably, the peak regulation amount of the S3 agent reaches 38 units, and the system prediction error MAE (Mean Absolute Error) remains stable at below 0.08 after 20 iterations. The load fluctuation experiment further shows that collaborative optimization can narrow the normalized load fluctuation range to  $\pm 0.15$  and increase the unit load resource utilization rate by 12%, confirming the rapid convergence ability and dynamic balance advantages of this method under extreme disasters.

**Keywords:** Typhoon disaster; Integrated energy system; Multi-agent collaboration; Distributed optimization; Resilience improvement.

Received: 10 September 2025; Revised: 07 November 2025; Accepted: 23 November 2025

Article Type: Research article.

## 1. Introduction

Typhoons are among the most destructive natural disasters in the world, and their strong winds, rainstorms, and secondary disasters pose severe challenges to the safe and stable operation of energy systems.<sup>[1,2]</sup> By virtue of the combined effect of strong wind, rainstorm and storm surge, typhoon has a multi-dimensional impact on the whole chain of power generation, transmission and consumption of the integrated energy system. Its impact mechanism mainly focuses on the three core issues of equipment failure, network congestion and load mutation: in terms of equipment failure, strong wind can cause the wind turbine unit to break, photovoltaic module to

be damaged, rainstorm can cause water accumulation in the thermal power plant, resulting in insulation failure, transmission line icing and collapse, tower toppling, outdoor energy storage cabin short circuit, and emergency generator can not be started due to water ingress; In terms of network congestion, strong wind may blow down foreign matters and hit the gas pipeline, resulting in a sharp drop in pressure. rainstorm will wash out the oil and gas transmission pipeline network, submerge the power substation, and interrupt the energy transmission channel; In terms of sudden load changes, power outages caused by typhoons can lead to a sharp increase in emergency lighting, temporary communication equipment, drainage pumps, and other loads. At the same time, industrial and commercial production loads are significantly reduced due to production shutdowns, resulting in an imbalance between load supply and demand, ultimately posing a threat to the safe and stable operation of the system. In response to typhoon events, the traditional single-energy system's independent regulation mode has many shortcomings in

<sup>1</sup>State Grid Shanghai Municipal Electric Power Company, Shanghai, 200122, China

<sup>2</sup>Northeast Electric Power University, Jilin, 132012, China

<sup>3</sup>China Electric Power Research Institute, Beijing, 100192, China

<sup>4</sup>School of Information Engineering, Nanchang University, Nanchang, 330031, China

complex dynamic environments, such as uncertain output of renewable energy, complex energy interactions, and difficulties in multi-objective optimization. The integrated energy multi-agent collaborative optimization regulation method can effectively improve the reliability, economy, and environmental friendliness of the energy system.<sup>[3-5]</sup> The integrated energy system offers a new technical path for enhancing the reliability and flexibility of energy supply by coupling multiple energy flows, such as electricity, gas, heat, and cold. However, its multi-energy complementary characteristics also present key issues, including the superposition of multi-source uncertainty and difficulties in cross-domain collaboration during typhoon situations.<sup>[6]</sup> In this context, achieving dynamic balance and rapid recovery of the integrated energy system during a typhoon event through a multi-agent collaborative optimization control method has become a pressing scientific problem in the field of energy system resilience construction.

As a distributed autonomous decision-making framework, a multi-agent system can effectively cope with the challenges of scattered information, diverse decision-making subjects, and dynamic environment changes in complex systems through cooperation among multiple agents with perception, communication, and decision-making capabilities. In the integrated energy system, each energy subsystem or key node can be regarded as an agent with independent optimization objectives, which achieves global coordination through local observation and interaction, thereby maintaining the overall stability of the system under uncertain conditions caused by typhoons.<sup>[7]</sup> Compared to the centralized control method, multi-agent collaborative optimization can reduce the computational burden of the central controller, improve the system's response speed to local faults, and enhance overall robustness through a distributed decision mechanism.<sup>[8,9]</sup> However, when dealing with extreme events such as typhoons, the existing research mostly focuses on emergency dispatching or static risk assessment of a single energy form, lacking the deep integration of multi-energy flow coupling dynamic characteristics and multi-agent interaction mechanism, especially in the scenario of time-varying typhoon intensity and significant spatial heterogeneity of disaster impact, the design of collaborative strategy among agents still faces many theoretical gaps and technical bottlenecks.<sup>[10]</sup>

The suddenness and destructiveness of typhoon events lead to high nonlinearity and strong uncertainty in the operating

environment of energy systems, making it difficult for traditional static optimization models based on historical data to accurately describe the real-time risk dynamics during typhoon evolution.<sup>[11,12]</sup> The multi-agent collaborative optimization control method needs to comprehensively consider multi-dimensional factors such as energy network topology, user demand response characteristics, spatiotemporal law of disaster propagation, and multi-energy flow coupling constraints, and dynamically adjust the operating parameters of key links such as power generation dispatching, load distribution, energy storage charging and discharging, and multi-energy conversion through information sharing and strategy iteration among agents.<sup>[13]</sup> In this process, the agent's decision-making not only depends on local observation information but also requires sensing the state changes of neighboring agents through the communication mechanism, and then forming a collaborative regulation strategy that considers both local interests and global optimality.<sup>[14]</sup> In addition, energy system regulation in typhoon scenarios also needs to strike a balance between safety and economic considerations. While ensuring power supply to critical loads, it also minimizes energy supply interruption losses and system recovery costs. This hinders the negotiation mechanism between multi-agents, and the optimization algorithm design imposes higher requirements.

In view of the above challenges, this study is devoted to exploring the comprehensive energy multi-agent collaborative optimization control method for typhoon events. By constructing a multi-agent distributed decision-making framework, the dynamic response law of a multi-energy flow coupling system under extreme disaster conditions is revealed, and a collaborative optimization strategy that considers real-time and robustness is proposed. The research will focus on the interaction mode between agents, the information transmission mechanisms, and adaptive decision-making methods in uncertain environments, aiming to provide theoretical support and technical solutions for enhancing the resilience level of integrated energy systems in extreme events, such as typhoons. Through the innovative application of multi-agent collaborative optimization control methods, it is expected to achieve rapid recovery and efficient operation of the energy system following typhoons, thereby laying a scientific foundation for the construction of highly resilient, comprehensive energy networks in the future.

## 2. Theoretical basis of multi-agent collaborative optimization control under typhoon disturbance

### 2.1 Integrated energy system

<sup>5</sup>Songyuan Power Supply Company, State Grid Jilin Electric Power Co., Ltd., Songyuan, 138099, China

<sup>#</sup>Note: State Grid Shanghai Municipal Electric Power Company and Northeast Electric Power University are co-first affiliations.

\*Email: Ydjian1015@163.com (Dejian Yang)

Faced with the challenges of excessive carbon emissions and the integration of new energy grids, regional integrated energy systems (RIES) offer solutions through multi-energy collaborative optimization.<sup>[15,16]</sup> Based on the concept of energy cascade utilization, the system is equipped with a variety of energy carriers and establishes a multi-energy complementary supply system, including cold, heat, electricity, and gas. This optimizes energy efficiency, improves the utilization of renewable energy, and reduces carbon emissions.

The RIES architecture centers on the power system as its core, integrating wind energy, solar energy, natural gas, and other energy sources, and combining the thermal system with the gas network to form an integrated energy supply system.<sup>[17]</sup> It consists of three main parts: the energy input part, which is mainly composed of wind power generation and solar panels; The energy conversion center uses gas engine, electro-thermal converter and electricity-to-gas technology to realize the conversion between different energy forms; And energy storage and buffer part, including battery pack, thermal energy storage and hydrogen storage facility, for regulating energy and ensuring the balance between energy supply and demand.<sup>[18]</sup> The energy network dynamically matches the risk of equipment failure through the correlation function of "wind

speed equipment failure rate", based on three levels: wind speed below the sensitivity threshold, between the sensitivity and extreme tolerance thresholds, and reaching the extreme tolerance value. Different equipment thresholds are calibrated based on historical data; The load model introduces a typhoon warning demand response coefficient, combined with the flexibility of warning levels and load types, to achieve non essential load reduction and transferable load spatiotemporal adjustment. At the same time, the system constraint boundaries are updated accordingly, incorporating device capacity attenuation, network topology changes, and adjusted load demands to form a quantitative constraint framework.

The technological innovation of this system is reflected in three levels: first, it integrates carbon capture and hydrogen fuel cells to form a clean energy chain; Secondly, power-to-gas technology is used to convert excess electricity into storable gas to solve the instability of new energy; Finally, an energy cascade utilization model is constructed to improve the overall energy efficiency, which is significantly superior to the traditional model.<sup>[19,20]</sup> This design reduces energy bills and provides a technical example for the construction of low-carbon energy infrastructure.<sup>[21]</sup> The comprehensive energy model framework structure of the system is shown in Fig. 1.

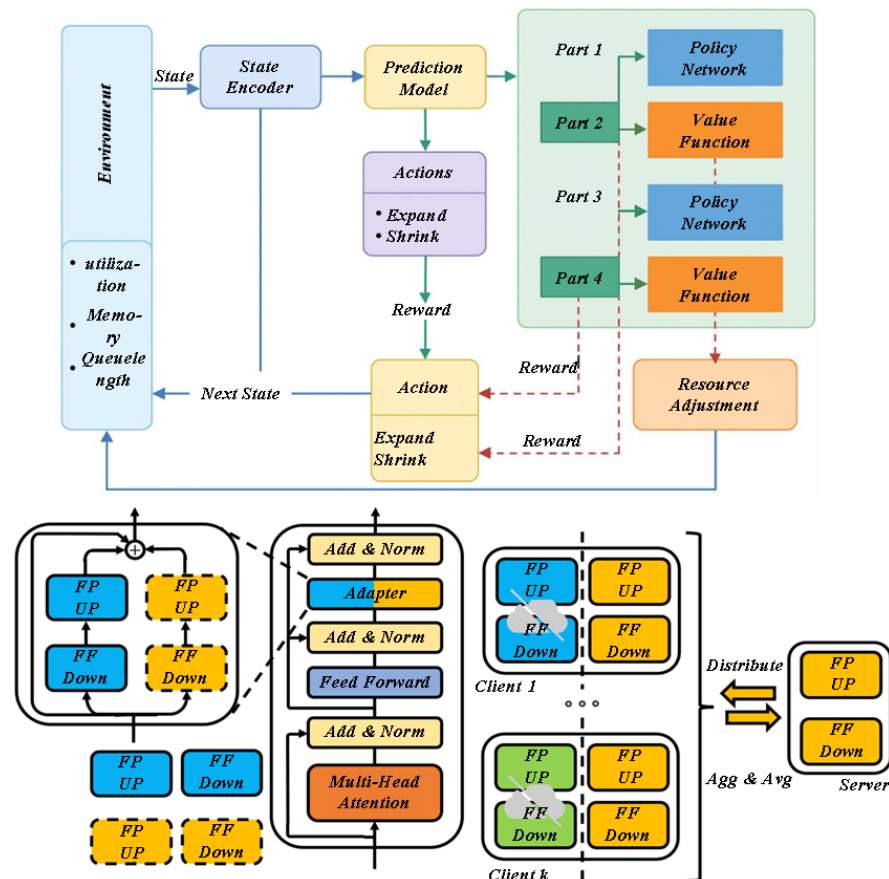


Fig. 1: Framework structure of integrated energy system model.

## 2.2 Definition of typhoon disaster concept

A typhoon is a strong tropical cyclone formed in the tropical ocean (sea temperature  $\geq 26$  °C). According to the maximum wind force in the center, it can be divided into tropical depression, tropical storm, severe tropical storm and typhoon. Located on the northwest Pacific coast, China is one of the countries most seriously affected by typhoons in the world. There are about 27 typhoons every year, of which about a quarter will affect China's coastal provinces (such as Hainan, Fujian, Guangdong, Guangxi, etc.).

A typhoon disaster is a compound meteorological disaster formed by the interaction of natural disaster factors, such as strong winds, rainstorms, and storm surges, with the human social system. It has the characteristics of a wide influence range, numerous secondary disasters, and strong destructive power.<sup>[22,23]</sup> The severity of the disaster depends not only on the intensity and path of the typhoon itself, but also closely related to social vulnerability factors such as population density, economic structure, and infrastructure resilience in the affected area.

From the perspective of disaster economics, although typhoons bring casualties, property losses and ecological damage, they also have certain resource attributes, such as alleviating drought and replenishing water resources. However, at the level of safe operation of the energy system, a typhoon is mainly regarded as a highly destructive extreme weather event, and its chain impact on multi-energy flow coupling systems, such as electricity, gas, and heat, is particularly prominent. It is urgent to improve system resilience through coordinated regulation.<sup>[24-26]</sup>

## 2.3 Multi-agent system

A Multi-Agent System (MAS) is a distributed computing framework composed of multiple agents with autonomous perception, communication, and decision-making capabilities. It is suitable for dealing with complex system optimization problems involving scattered information, a dynamic environment, and heterogeneous agents.<sup>[27-30]</sup> In the context of integrated energy systems, MAS facilitates the organic combination of local optimization and global coordination by modelling energy subsystems or key nodes, such as electricity, gas, and heat, as intelligent agents. It is especially suitable for multi-energy flow systems under extreme events, such as typhoons, for dynamic regulation and control.<sup>[31]</sup>

Compared with traditional centralized control, MAS shows significant advantages in dealing with typhoon disasters: its distributed architecture can avoid single-point failure and improve system robustness; The local decision-making ability of the agent can speed up the response to fault events; Through

the communication and negotiation mechanism between agents, complementary coordination across energy forms can be achieved, and overall resilience can be enhanced.<sup>[32]</sup> To further improve resource efficiency, event-triggered control is introduced into the MAS collaborative process, enabling agents to communicate and update policies only when the system state deviates from a predefined threshold, thereby ensuring optimal performance while minimizing redundant interactions.

Based on the MAS framework, this article constructs a collaborative control system that includes hazard factors, hazard bearing entities, decision support, and early warning evaluation entities.<sup>[33]</sup> The system achieves the recognition and inference of typhoon disaster chains, real-time perception of operational status, and generates and evaluates multi-objective optimization strategies through hierarchical collaboration and information fusion among intelligent agents. It provides guarantees for the rapid recovery and stable operation of integrated energy systems under extreme weather conditions, as well as distributed decision support. Among them, the information exchange between intelligent agents follows a specific protocol: when the typhoon intensity exceeds the preset threshold, the real-time data collected by the perception layer device will be converted into a unified format according to standardized specifications, and time stamps, device numbers, and credibility ratings will be attached; The risk factor agent synchronously transmits standardized data to the disaster bearing agent and decision support agent through the MQTT protocol. The disaster bearing agent provides short-term feedback to receive confirmation, while the decision support agent sends back preliminary risk assessment results through the WebSocket protocol, forming a closed-loop interaction to ensure information synchronization.<sup>[34]</sup>

This paper constructs a closed-loop error tracking system for the consistency tracking problem of heterogeneous nonlinear multi-agent systems, and derives the consistency conditions using the Lyapunov Krasovskii function. A design strategy for the gain matrix of the consistency controller is proposed. This strategy ensures that in the collaborative control system, even if there are heterogeneous and nonlinear characteristics among various agents, they can achieve consistent tracking of their states, providing a stable control foundation for hierarchical collaboration; At the same time, in order to improve the efficiency of system operation, an event triggered control strategy is introduced, which determines the timing of sampling and control updates based on preset event triggering conditions. When the system state approaches equilibrium, meaningless repeated sampling is not performed if the triggering conditions are not met, effectively reducing

the amount of data transmission and computing resource consumption, and further adapting to the dual requirements of real-time and economy of comprehensive energy systems in typhoon emergency scenarios. Introduce time-delay parameters and construct Lyapunov Krasovskii candidate functions containing system state variables and time-delay state integral terms, ensuring that the functions satisfy positive definite conditions; Subsequently, the derivative of the candidate function is calculated along the system trajectory, combined with the typhoon disturbance boundary conditions and multi-agent consensus protocol, and the derivative expression is simplified using tools such as matrix inequality transformation and Schur complement lemma; Finally, sufficient conditions are derived to make the derivative negative definite, verifying the asymptotic stability of the system's coordinated control under the influence of typhoon disturbance and time lag, and completing the derivation of the function core.<sup>[35]</sup>

### 3. Construction of a typhoon event-driven multi-agent collaborative optimization regulation model for integrated energy

#### 3.1 Integrated energy multi-agent network construction and social network analysis

This study first processes the data of energy multi-agents and extracts geographic information from them. Then, based on the geographic information, a regional association data matrix is constructed. The matrix contains a total of 398, 652, 1247 and 2214 contact pairs, respectively. After completing the classification assignment of energy multi-agents, we calculate the connection strength between each node according to Eq. (1).

$$T_{ij} = \sum_{m=1}^n V_{if} \times V_{jf} \quad (1)$$

$T_{ij}$  represents the connection strength between cities  $i$  and  $j$ ;  $m$  is the number of energy multi-agents shared by cities  $i$  and  $j$ ;  $V_{if}$  and  $V_{jf}$  represent the score of firm  $f$  in cities  $i$  and  $j$ , respectively.

Social network analysis (SNA) aims to analyze the network structure and node relationship, so as to reveal the difference between the overall network state and node status. In this study, we use network density and average path length to characterize the structure and evolution characteristics of energy multi-agent networks, and use weighted centrality to characterize node characteristics. Specifically, network density measures the tightness of connections between cities in an enterprise network, and its calculation Eq. (2) is as follows:

$$D_n = \frac{L}{[n(n-1)]} \quad (2)$$

$D_n$  represents the density of the energy multi-agent network,  $L$  is the actual number of contacts within the network, and  $n$  represents the total number of cities. Network density ranges from 0 to 1, with values close to 1 indicating a dense network and values close to 0 indicating a sparse network.

The average path length is used to measure network transmission efficiency and reflect connectivity. A short path indicates good connectivity, while a long path indicates poor connectivity. The calculation process is shown in Eq. (3).

$$L = \frac{1}{n(n-1)} \sum_{i \neq j} d_{ij} \quad (3)$$

where  $L$  represents the average shortest path length of the energy multi-agent network,  $n$  is the number of cities, and  $d_{ij}$  is the path distance from city  $i$  to city  $j$ .

The weighted centrality evaluates the importance of network nodes. The larger the value, the stronger the linkage ability of the nodes, and the more core the city is in the network. In directed networks, it is divided into weighted out degrees and weighted in degrees. Weighted out degree measures urban radiation, and weighted in degree measures urban attractiveness and cohesion. The calculation is shown in Eq. (4)-(6):

$$C_{Di} = C_{Di}(in) + C_{Di}(out) \quad (4)$$

$$C_{Di}(in) = \sum_{j=1}^n W_{ij} r_{ij}(in) \quad (5)$$

$$C_{Di}(out) = \sum_{j=1}^n W_{ij} r_{ij}(out) \quad (6)$$

$C_{Di}$  represents the weighted degree centrality of city node  $i$ , and  $C_{Di}(in)$  and  $C_{Di}(out)$  represent the weighted point-in degree and weighted point-out degree of city node  $i$  respectively;  $W_{ij}$  is the weight of the edge between city node  $i$  and city node  $j$ ;  $r_{ij}$  is the number of inter-city edges;  $n$  is the total number of nodes within the network.

Intermediary centrality reflects the control power of a city as an intermediary in the energy multi-agent network. The higher its value, the stronger the control ability of the city over the enterprise connections between other cities. The calculation Eq. (7) is as follows:

$$C_B(i) = \sum_{j=1; k=1; j \neq k \neq i}^n \frac{N_{jk}(i)}{N_{jk}} \quad (7)$$

$N_{jk}$  represents the number of shortest paths between city nodes  $j$  and  $k$  in the enterprise network;  $N_{jk}(i)$  denotes the number of nodes in cities  $i$  and  $k$  through which these paths pass.

Efficiency correction formula for core energy equipment under different typhoon conditions (variables calibrated according to typhoon level): For wind turbines, between rated wind speed (12-15m/s) and cut-out wind speed (25-30m/s),  $\eta_{wind}=\eta_{w0}[1-\alpha_1(v-v_{rated})^2/(v_{cut}-v_{rated})^2]$  ( $\eta_{w0}=0.85-0.92, \alpha_1=0.8-1.2$ ), when the cut-out wind speed exceeds the threshold,  $\eta_{wind}=0$ , and wind direction correction is added,  $\eta_{dir}=1-\beta_1\sin^2\theta$  ( $\beta_1=0.05-0.12$ ). The total comprehensive  $\eta_{wind}=\eta_{wind}\times\eta_{dir}$ ; Photovoltaic modules, when the wind speed is  $\leq 25\text{m/s}$ ,  $\eta_{pv}=\eta_{p0}e^{-(\gamma_1v)}$  ( $\eta_{p0}=0.18-0.25, \gamma_1=0.015-0.03, \delta_1=0.002-0.005$ ), and when the wind speed exceeds 25m/s,  $\eta_{pv}=0.3$ ; When the wind speed of the energy storage inverter is  $\leq 30\text{m/s}$  and the rainfall is  $\leq 50\text{mm/h}$ ,  $\eta_{ess}=\eta_{e0}[1-\varepsilon_1(v^{0.8}+r^{0.5})]$  ( $\eta_{e0}=0.93-0.97, \varepsilon_1=0.001-0.003$ ), and when this condition is exceeded,  $\eta_{ess}=0.65$ .

Real time collection of typhoon parameters by various device agents, inputting them into corresponding correction formulas to calculate dynamic efficiency, and transmitting efficiency data to the control agent; The regulation agent aims to balance regional energy supply and demand and ensure safe operation of equipment. It constructs an optimization objective function with modified efficiency constraints and generates regulation strategies through distributed iteration of multi-agent systems. At the same time, each device agent dynamically updates the efficiency correction value and model optimization parameters based on the feedback of regulation instructions, forming a closed-loop integrated mechanism of "parameter collection efficiency correction model optimization instruction execution feedback update" to improve the accuracy and response speed of comprehensive energy system regulation during typhoons.

As the core carrier of energy cascade utilization and multi energy complementarity in integrated energy systems, the modeling of multi energy coupling equipment needs to start from the energy conversion mechanism, reveal the inherent coupling law between input and output energy flow, and incorporate dynamic characteristic constraints under extreme working conditions. The electrical thermal coupling characteristics of gas turbines are reflected as follows: taking natural gas chemical energy as input, synchronously outputting electrical energy and waste heat energy through combustion power generation process. The output relationship between the two is determined by energy conservation and equipment operating efficiency - power generation efficiency dominates the proportion of electrical energy conversion, while waste heat recovery efficiency affects the scale of thermal energy output. This coupling relationship dynamically changes with load rate. Under extreme conditions such as typhoons, environmental parameter fluctuations will further cause the efficiency curve to shift, and its nonlinear

characteristics need to be reflected through a working condition correction mechanism. The thermal cooling coupling of lithium bromide absorption refrigeration machine is essentially the energy quality conversion driven by thermal energy. Its core is the dependence of refrigeration coefficient on heat source parameters and environmental conditions: thermal energy input is converted into cold energy output through thermal cycle, while the high temperature and high humidity environment during typhoons will reduce the cycle thermal efficiency, causing the refrigeration coefficient to exhibit attenuation characteristics. At the same time, the cold energy output needs to be constrained by the minimum/maximum output determined by the physical performance of the equipment, forming boundary conditions for thermal cooling conversion. The electric gas coupling of electric to gas conversion equipment is based on the energy conversion logic of electrolysis reaction. The input of electric energy is converted into natural gas chemical energy through electrochemical process, and its conversion efficiency depends not only on the performance of the equipment itself, but also on the stability of the input electric power. The grid fluctuations caused by typhoons may lead to instability of the electrolysis process, so power mutation rate constraints need to be included in the model to reflect the dynamic safety boundary of electric to gas conversion. The above device model provides underlying theoretical support for multi-agent collaborative optimization and control in typhoon scenarios by quantifying the physical laws of energy flow coupling and the constraint mechanism under extreme working conditions, ensuring that each subject can accurately grasp the feasibility and economic boundaries of multi energy flow conversion in the decision-making process.

The power network takes the balance of active and reactive power at each node as its core element. In addition to integrating the output of distributed power sources such as photovoltaics and wind power, the charging and discharging capacity of energy storage equipment, and local power loads, it also converts the energy of the gas network into electrical energy through the power generation of gas turbines, thereby achieving power transfer between the electricity and gas networks. The key point of the gas network is the balance of gas flow at each node. While meeting its own gas load and the filling and discharging needs of gas storage equipment, the gas consumption of gas turbines is used to reverse the energy demand of the power network, thereby forming a closed-loop system of energy interaction between the two. The thermal network revolves around the balance of heat flow at each node. On the one hand, waste heat utilization equipment is used to recover the waste heat generated during the gas turbine power

generation process and convert it into heat energy. On the other hand, electric boilers consume electrical energy to achieve heating, and energy transfer channels for electric thermal and gas thermal networks are constructed separately. Ultimately, the three major networks form a collaborative and complementary energy flow system by leveraging the energy conversion and demand reception of core devices.

### 3.2 Multi-agent collaborative optimization model

In the model constructed in this study, agents are divided into five categories: interface agent, hazard factor agent, disaster-bearing agent, decision support agent and early warning evaluation agent. These five types of agents constitute five functional layers, which are connected through event mechanisms to form a loosely coupled open framework system. Interface agent displays prediction results and evaluation; Disaster-bearing agent and database form a disaster information management platform; The core business consists of a disaster agent layer, a disaster-bearing agent layer and a database to realize the coupling prediction of multiple disasters in the disaster chain; The decision support layer provides two kinds of decision support tools, including the timing control agent at the system level and the encapsulation decision algorithm tool; The evaluation agent is customized according to the needs, and mainly evaluates the early warning indicators of natural disasters, including casualties, economic losses and environmental damage. The multi-agent collaborative optimization model is shown in Fig. 2. The

typhoon specific sub objective is to minimize the loss of load to ensure critical load power supply, maximize the reliability of emergency power supply, and strengthen the continuous supply of emergency power. Multiple typical scenarios containing weak, strong, and super typhoons are generated through Monte Carlo simulation or K-means clustering to characterize the uncertainty of typhoons such as equipment failure probability, load fluctuation, and renewable energy output impact. Multiple scenario objectives are integrated with scenario probability as weights to form a stochastic programming model; Clarify the roles of intelligent agents such as power grid, gas grid, energy storage, and emergency response, and implement a collaborative process of "global coordination agent releases goals - each agent solves sub problems - consistency algorithm eliminates conflicts" to achieve global optimization under constraints such as multi energy balance and resource scheduling, providing resilience control solutions for comprehensive energy systems to cope with typhoons.

Agents interact to realize communication. The interface agent inputs catastrophic parameters, activates the catastrophic agent, and feeds back the features to the user; Disaster agent and disaster-bearing agent cooperate to simulate disaster chain; During prediction, the agent makes a request to the decision support agent to complete the prediction together; The disaster-bearing agent manages the database status; Assessment agents assess disaster impacts and display early warnings through interface agents.

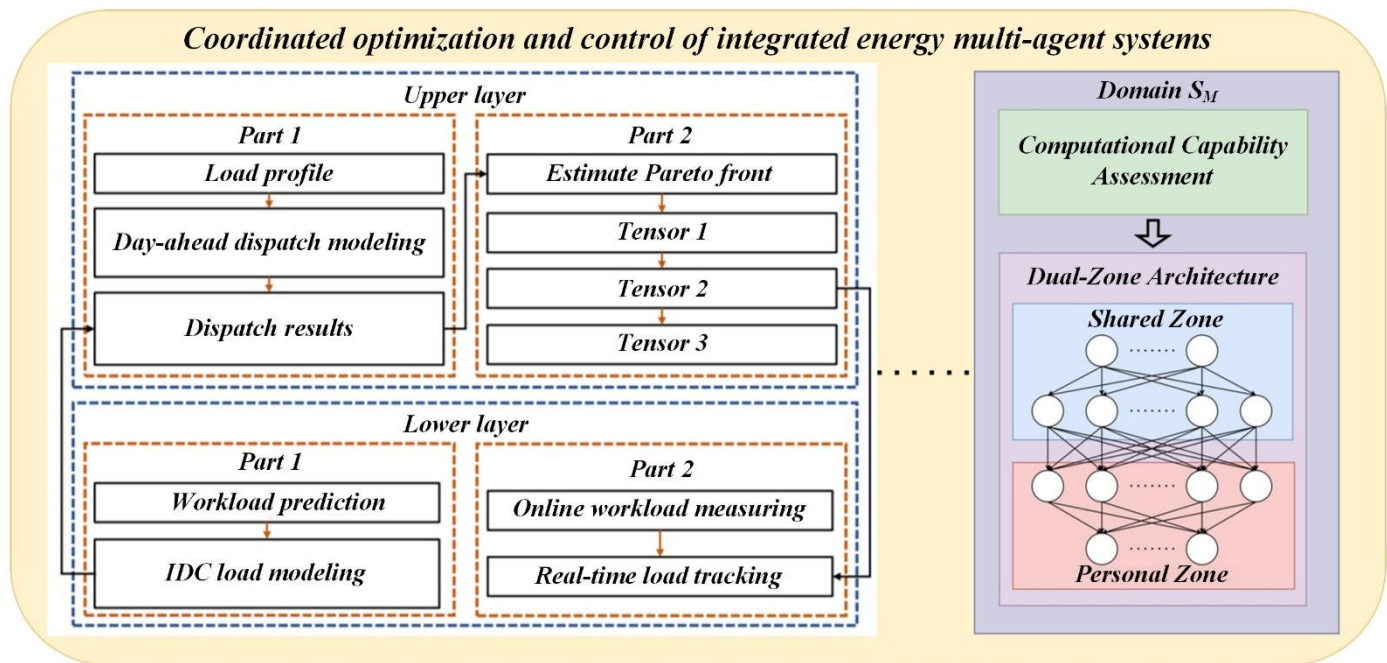


Fig. 2: Model implementation framework.

The objective function of comprehensive energy multi-agent collaborative optimization under typhoon events is constructed around "safety economy environmental protection": the safety objective focuses on reducing operational deviations of key nodes, improving power supply reliability, and reducing load outage losses; The economic objective aims to minimize the comprehensive operating costs including fuel, electricity purchase, and emergency maintenance costs, while taking into account demand response benefits; The core of environmental protection goals is to improve the consumption rate of renewable energy, and the three types of goals are integrated into a single objective optimization model through typhoon risk weight coefficients and weighted sum method. The key constraint conditions include: multi energy flow power balance constraint, which needs to be combined with the fluctuation of new energy output caused by typhoons, and maintain the balance of electricity, heat, and gas rates through source grid load storage interaction; Equipment operation constraints, clarifying the operating limits of wind power, energy storage, traditional units and other equipment; Safe operation constraints ensure stable grid voltage, control interruptible load shedding, and meet energy network safety limits. At the same time, event triggering mechanisms are used to reduce redundant interactions, and distributed optimization algorithms are used to achieve iterative convergence and ensure stable system operation.

### 3.3 Negotiation strategy among multiple agents and distributed optimization algorithm embedding

In the typhoon event-driven, integrated energy, multi-agent collaborative optimization and control scenario, the negotiation strategy between multiple agents must combine the dynamic characteristics of typhoon disasters with the operating constraints of integrated energy systems to establish a distributed decision-making mechanism with anti-interference capabilities. Firstly, based on the weighted centrality and intermediary centrality of nodes in social network analysis, core agents in the network are identified. These core agents lead the initiation of negotiations and conflict coordination, and the communication complexity of large-scale agent networks is reduced through a hierarchical negotiation strategy. During the negotiation process, an information interaction mechanism based on event triggering is introduced. When the typhoon disturbance causes the deviation between energy supply and demand to exceed the preset threshold, real-time data sharing between agents is triggered to prevent the unnecessary consumption of communication resources. To address the heterogeneity of

different types of agents, a multi-attribute negotiation protocol is designed to transform energy supply reliability, economy, disaster risk, and other indicators into a unified utility function. The Pareto optimal negotiation solution is then solved using the Nash bargaining model. In the Nash bargaining model for comprehensive energy under typhoons, the utility functions of three types of intelligent agents revolve around "profit minus cost": the supply side utility is the sum of electricity sales revenue and reserve subsidies, minus the cost and transmission losses adjusted due to the decrease in typhoon output; The utility of the storage side is to save money by charging during low periods and earn money by discharging during high periods or typhoons, minus the additional costs of equipment maintenance and emergency adjustments; The utility on the demand side is the benefit of meeting electricity demand, minus the cost of purchasing electricity and the loss of coordinating the regulation of less electricity consumption.

The embedding of a distributed optimization algorithm requires solving the dynamic coupling and real-time requirements of a multi-agent system in a typhoon scenario. Based on the consensus algorithm theory, the traditional event triggering mechanism is enhanced, and adaptive triggering conditions integrating typhoon warning levels are designed. When the typhoon intensity level increases, the condition monitoring period for event triggering is automatically shortened, thereby improving the algorithm's response speed to extreme working conditions. Aiming at the mixed integer nonlinear characteristics of an integrated energy system, the alternating direction multiplier method (ADMM) is used for distributed optimization decomposition, and the global regulation objective is disassembled into local sub-problems of each agent, and the sub-problems are solved collaboratively by iterative update of dual variables. At the same time, the robust optimization concept is introduced to address the uncertainty in typhoon parameters, and a risk penalty term is added to the objective function. The convergence of the algorithm under parameter perturbation is then proved using Lyapunov-Krasovskii stability theory. By embedding the gradient information of the utility function into the negotiation strategy during the iterative process of the optimization algorithm, dynamic matching between negotiation outcomes and optimization variables was achieved, ultimately realizing the goals of multi-agent collaborative decision-making and global optimization under typhoon disturbances.

### 3.4 Dynamic update of model parameters

Using the functions of attribute extraction, regional statistics and raster calculation of ArcGIS, the risk weighting coefficient of the area where the demand point is located can be calculated.

Using the data, this study divides the use types into impermeable surface and non-impermeable surface, and calculates the risk coefficient: extracting these two types in the demand area, and calculating the risk index according to the disaster risk level and land use proportion; Different weights are assigned to these two types of land, and the risk weights of demand points are obtained by weighting calculation. The calculation model is shown in Eq. (8), where  $q_i$  is the hazard index of the impermeable surface in the demand area and  $k_{qi}$  is its weight;  $g_i$  is the hazard index of the non-impermeable surface in the demand area, and  $k_{gi}$  is its weight;  $D_i$  is the risk weight coefficient of demand region  $i$ .

$$D_i = k_{qi} \cdot q_i + k_{gi} \cdot g_i \quad (8)$$

Use EXCEL, ArcGIS and other tools to analyze the data, and calculate the results. In the analysis, the influence of population and economy on demand is considered, and the demand coefficient is calculated instead of the exact demand. In Eq. (9),  $F_i$  represents the demand coefficient of demand region  $i$ ,  $p_i$  and  $e_i$  are the demand population index and economic index respectively, and  $k_{pi}$  and  $k_{ei}$  are their weights.

$$F_i = k_{ei} \cdot e_i + k_{pi} \cdot p_i \quad (9)$$

Determine the population index of  $i$  in the city according to the number of inhabitants and the proportion of the population in the demand area  $i$ . The population index is high, and the demand for emergency supplies is large. Eq. (10) shows that  $p_i$  is the population index of demand region  $i$ ,  $p_i'$  is the demand population of  $i$ , and  $\sum_{n=1}^N p_i'$  is the total demand population.

$$p_i = \frac{p_i'}{\sum_{i=1}^N p_i'} \quad (10)$$

The economic index shows the economic importance of the demand area, and the greater the value, the more serious the damage during the disaster. In Eq. (11),  $e_i$  is the economic index of demand region  $i$ ,  $e_i'$  is the average GDP per land, and  $e_{i'_{min}}$  and  $e_{i'_{max}}$  are the minimum and maximum values of  $e_i'$ , respectively.

$$e_i = 0.5 + \frac{e_i' - e_{i'_{min}}}{e_{i'_{max}} - e_{i'_{min}}} \quad (11)$$

After obtaining the risk weight coefficient  $D_i$  and the demand weight coefficient  $F_i$ , the emergency weight coefficient can be calculated according to the index weight method, as shown in Eq. (12). Among them,  $W_i$  is the contingency weight coefficient,  $D_i$  is the risk weight coefficient, and  $kD_i$  is its weight;  $F_i$  is the demand weight coefficient and  $kF_i$  is its weight.

$$W_i = kD_i \cdot D_i + kF_i \cdot F_i \quad (12)$$

The coupling logic of "urban form energy demand" constitutes the core framework of demand side analysis, and its mechanism of action is reflected in the quantitative driving of energy demand by key indicators of urban form: firstly, the proportion of impermeable surfaces affects the cooling load intensity by regulating the regional microclimate - in high proportion areas, due to the enhanced heat island effect, the cooling demand significantly increases before and after typhoon passage (especially during high-temperature periods of sinking airflow), while in low proportion areas, the load fluctuation is smoother due to the thermal regulation effect of green spaces and water bodies; Secondly, the proportion of non impermeable surfaces affects the output of renewable energy by changing the efficiency of photovoltaic radiation reception - high proportion areas (such as open roofs and green spaces) have higher potential for photovoltaic utilization, which can reduce the dependence of energy demand on conventional energy, especially when energy supply is tight due to typhoons; Thirdly, population density and economic level jointly determine the priority weight of emergency energy use - rigid energy use in densely populated areas (such as residential areas and medical facilities) and key production energy use in economic core areas (such as industrial parks and commercial hubs) constitute the priority judgment criteria for multi-agent energy allocation.

Based on the above coupling logic, a "demand side feature regulation strategy" mapping model is constructed to transform the derived features of urban form into quantifiable parameters for optimizing the model: using the proportion of impermeable surfaces as a load forecasting correction factor, dynamically calibrating the cooling load forecasting results of different regions, and correcting the forecasting bias caused by microclimate differences; Using population density as the priority coefficient for multi energy collaborative energy supply, giving higher weight to high population density areas in energy dispatch constraints to ensure core energy demand; At the same time, the proportion of non impermeable surfaces and economic level are respectively used as the correction term for renewable energy output prediction and the adjustment term for emergency energy weight. The multi-agent optimization objective function is embedded to clarify the transmission path of each parameter from feature extraction to regulation decision-making, achieving deep coupling of urban form, energy demand and regulation strategy, and improving the optimization efficiency and emergency support capability of the comprehensive energy system in typhoon scenarios.

#### 4. Experiment

### 4.1 Example background and parameter settings

This study takes a typical industrial park along the coast as an example area. The park covers multiple industries such as manufacturing and research and development, and its energy demand presents a coupled characteristic of "electricity gas heat". During the typhoon season (July September), it often faces the risk of energy supply interruption caused by extreme weather, which is typical for conducting comprehensive energy regulation research. The energy network topology adopts a collaborative architecture of "IEEE 33 node distribution network+7-node natural gas pipeline network": the IEEE 33 node distribution network includes 32 feeders, 1 balancing node, and 32 load nodes, with a rated voltage of 12.66 kV, covering more than 90% of the power load in the park; The 7-node natural gas pipeline network includes 5 main pipelines, 2 gas source nodes (connecting the city gate station and LNG emergency storage station respectively), and 5 gas consumption nodes (corresponding to gas turbines, industrial boilers, and other equipment). The pipeline network is designed with a pressure of 4.0MPa to meet the gas supply needs of the park. The core equipment parameters are determined based on the measured data of mainstream commercial equipment in China, including three gas turbines with a rated power of 10MW (power generation efficiency of 38%, waste heat recovery efficiency of 85%), two sets of 20MWh/10MW lithium-ion battery energy storage systems (charge and discharge efficiency of 92%, deep discharge threshold of 20%), and one 5MW electric heating boiler (heating efficiency of 95%).

Scenario design is divided into benchmark scenario and typhoon scenario: In the benchmark scenario (no typhoon), the load data is based on the actual monitoring data of the non typhoon season of this type of park for 30 consecutive days in 2023 (peak power load of 28MW, valley value of 12MW, peak gas load of 1500m<sup>3</sup>/h, valley value of 800m<sup>3</sup>/h), and the meteorological data is taken from the self built meteorological station in the park (daily average wind speed of 2.5m/s, daily average temperature of 26 °C), simulating normal operating conditions; Typhoon scenarios are classified into three wind speed levels (10-12, 13-15, 16 and above) according to the "Tropical Cyclone Classification". Meteorological data is sourced from the historical typhoon dataset publicly available by the China Meteorological Administration (such as hourly wind speed and rainfall data during typical typhoons). Load data is adjusted based on the production adjustment rules of the park during typhoons (industrial load drops to 70% of normal level during 10-12 levels, and only 2MW emergency load is retained during shutdown at 16 levels and above), while considering the impact of typhoons on distributed photovoltaics (output reduction of 30% -80%) and transmission lines (possible tripping above 13 levels).

The simulation tool selected is MATLAB R2023a combined with YALMIP toolbox. The former supports efficient numerical calculation and visualization, while the latter is convenient for interfacing with CPLEX and other solvers to handle constraint conditions; The solving algorithm adopts an improved NSGA-II (Non-dominated Sorting Genetic Algorithm II), and the parameter settings have been

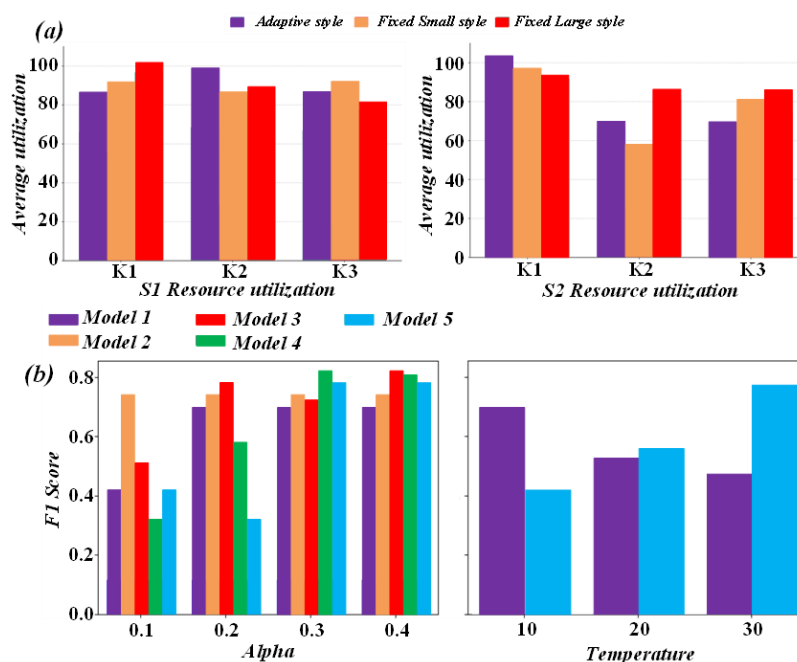


Fig. 3: S1 and S2 resource utilization rates of different models under different styles.

verified to be reasonable: population size of 100 (balancing efficiency and solution diversity), maximum iteration times of 200 (convergence error<1% after iteration), crossover probability of 0.8 (ensuring gene exchange), and mutation probability of 0.05 (maintaining diversity). This configuration is in the multi-objective optimization of "economy reliability environmental protection", which can control the duration of a single simulation within 30 minutes and obtain a uniformly distributed Pareto optimal solution, meeting the needs of comprehensive energy multi-agent collaborative regulation under typhoons.

### 4.2 Experimental results and analysis

Fig. 3 (a) shows the average resource utilization rates of S1 and S2 under K1-K3 conditions for adaptive style, fixed small style, and fixed large style during typhoon response. In S1, the utilization rate of fixed large style under K1 reaches 100%; In S2, the adaptive style utilization rate exceeds 95% in K1, while the fixed small style is only about 60% in K2. Fig.3 (b) shows the F1 scores of multiple models with Alpha parameters ranging from 0.1 to 0.4 and Temperature parameters of 10, 20, and 30. In the Alpha parameter experiment, Model 4 performed better when the F1 score reached around 0.8 at Alpha values of 0.3 and 0.4; In the temperature parameter experiment, Model 5 showed good performance with an F1 score close to 0.8 at a temperature of 30.

Fig. 4 shows the three-dimensional path of integrated energy multi-agent collaborative optimization regulation of seven models in response to typhoon events. The horizontal axis x, vertical axis y and vertical axis z represent different dimensional parameters respectively. The path of each model

is different, which is obvious in the interval of x about 5-7, y about 300-800, and z about 1.0-4.5, reflecting the difference of regulation strategies of different models.

Table 1 shows that in the simulated line fault scenario caused by typhoon, the voltage deviation of key nodes is large (average 0.17 p.u.) due to the independent response of each energy subsystem in conventional regulation; Multi-agent collaborative regulation dynamically adjusts the output and load demand of distributed power generation through the real-time interaction of source-grid-load-storage, significantly reducing the node voltage fluctuation, and the average deviation is reduced to 0.05 p.u., which verifies the effect of collaborative strategy on improving voltage stability.

**Table 1:** Comparison of voltage deviation of key nodes under different control strategies.

Regulation strategy	Node 1	Node 5	Node 10	Mean deviation (p.u.)
Routine regulation	0.12	0.18	0.21	0.17
Multi-agent collaborative regulation	0.03	0.05	0.06	0.05

Fig. 5 shows three ways to deal with typhoon events, with time (hours) on the horizontal axis and quantity on the vertical axis. Method 1 has a concentrated variation in quantity at about 12-14 hours; Method 2 quantity distribution is relatively scattered; Method 3 The quantity fluctuates frequently in each period. These data reflect the differences in the performance of different methods during typhoons.

Fig.6 shows the relevant indicators changing with time (0-5 days) under the two parameter settings of  $\Lambda = 1$  and  $\Lambda = 2$

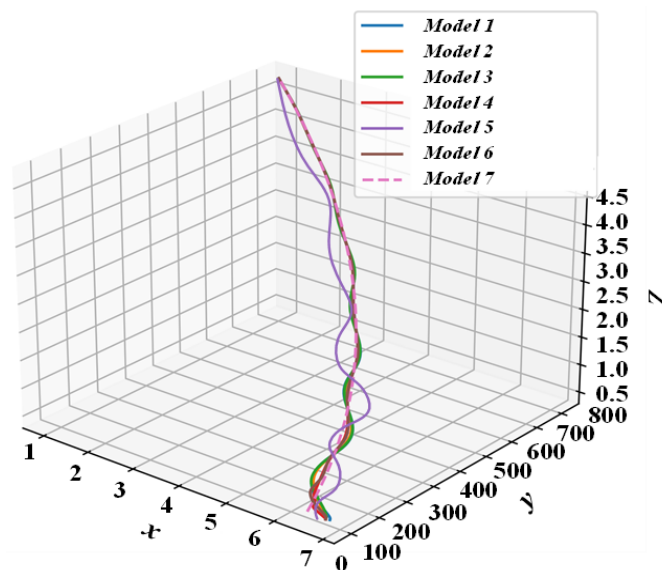


**Fig. 4:** Comparison of comprehensive energy multi-agent collaborative optimization control paths for typhoon events under different models.

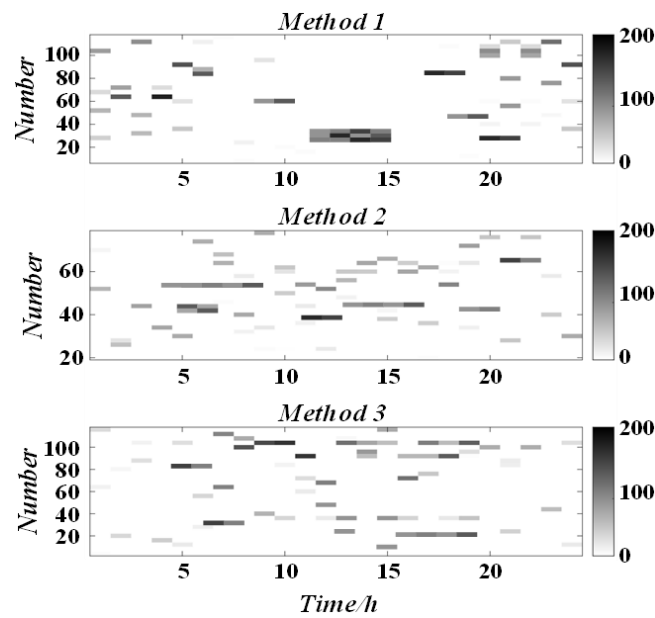


Fig. 5: Variation of comprehensive energy-related quantity over time during typhoon under different methods.

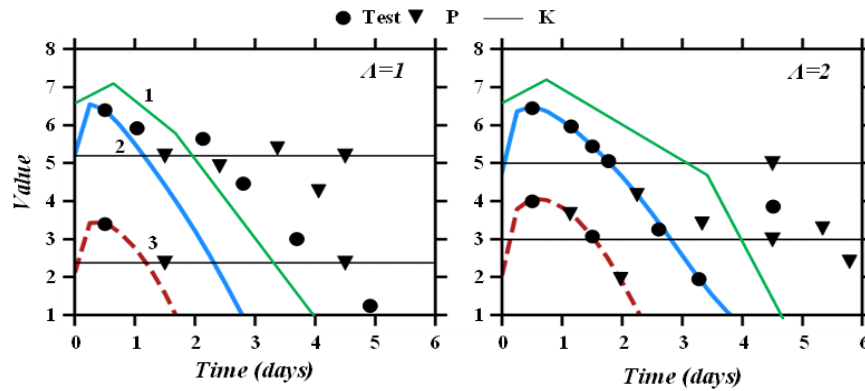


Fig. 6: Changes of key indicators of comprehensive energy during typhoon under different parameters.

Table 2: Operational benefits of integrated energy system under multi-agent collaborative control.

Index	Routine regulation	Multi-agent collaborative regulation	Lift rate
System power supply reliability (%)	82.3	95.6	16.00%
Renewable energy consumption rate (%)	68.5	89.2	21.70%
Comprehensive operating cost (yuan)	12,450	9,820	-21.10%

when dealing with typhoon events. The curves represent different models or parameters, and the scatter points are test data. It can be seen that with the passage of time, the index value shows a downward trend, and there are differences in the change rate under different  $\Lambda$  values.

Table 2 shows that for the extreme scenario of a typhoon lasting for 24 hours, multi-agent collaborative regulation improves power supply reliability by 16.0%, renewable energy consumption rate by 21.7%, and reduces reserve capacity redundancy through multi-energy complementation and demand-side response. Combined with wind and light abandonment losses, the comprehensive operating cost is

reduced by 21.1%, reflecting the economic and reliability advantages of collaborative optimization in typhoon events.

Fig. 7 shows the variation curve of a certain value of comprehensive energy with offset  $z$  under the experiment of detectable ratios (20%, 10% and 60%, 15%) of two different models. It can be seen that with the increase of offset, the value gradually increases, and the corresponding curves of different detectable proportions are obviously different, which can reflect the positive influence of model detection ability on regulation.

Fig. 8 shows the variation in average time to completion for Models 1-6 under Iteration S1-S4. The completion time of

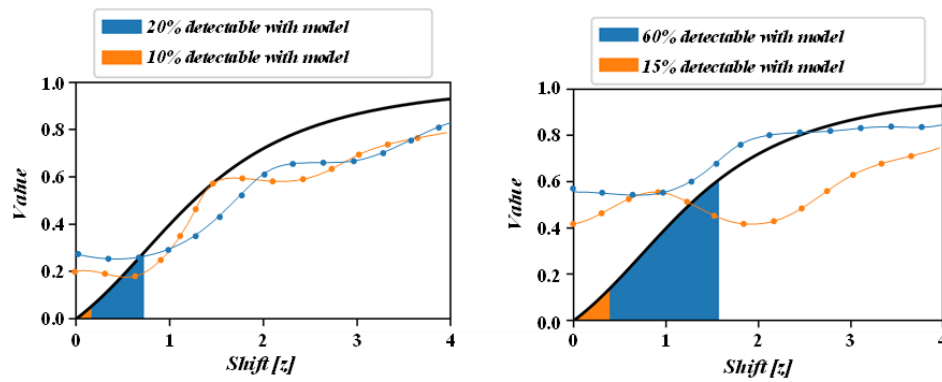


Fig. 7: Variation of comprehensive energy correlation values with offset under model detectable scale.

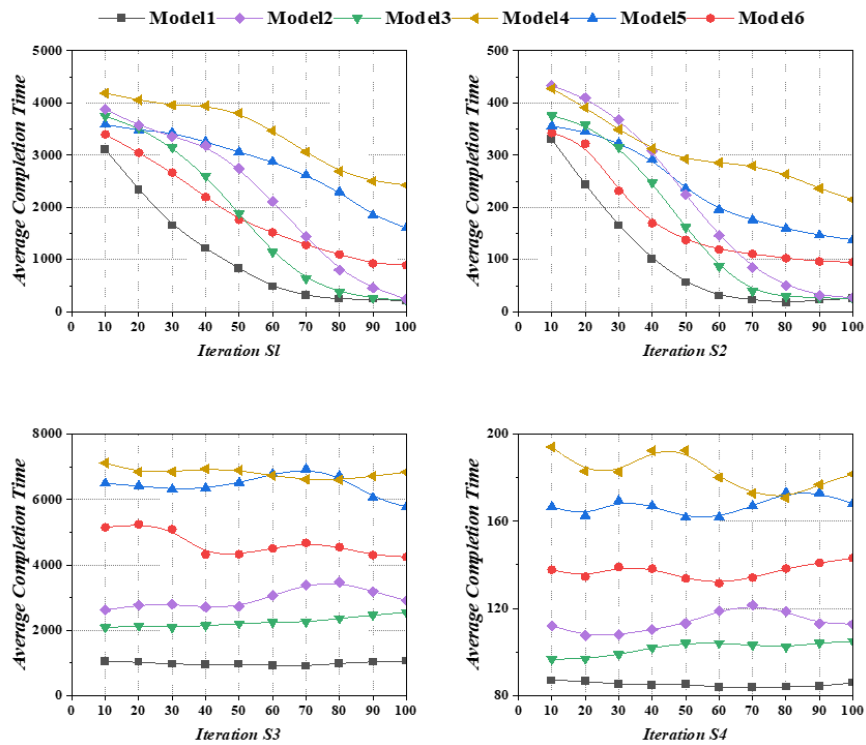


Fig. 8: Completion time performance of different models for integrated energy multi-agent collaborative optimization regulation under typhoon events.

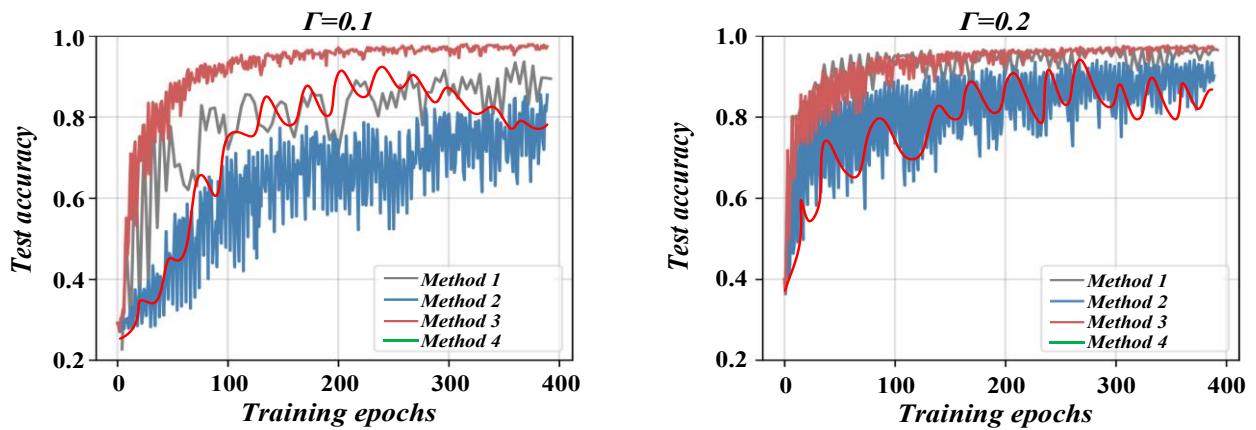


Fig. 9: Curves of test accuracy of four methods with training rounds under different  $\Gamma$  values.

each model in S1 and S2 decreases with iteration, while S3 and S4 show different fluctuation trends. For example, the completion time of Model 4 in S3 fluctuates between 6000 and 7000, reflecting the performance differences of different models in regulation.

Fig. 9 shows how the test accuracy of the four methods (Method 1-Method 4) changes with training rounds when  $\Gamma$  is 0.1 and 0.2, respectively. When  $\Gamma = 0.1$ , the test accuracy of Method 3 rises rapidly and finally stabilizes at a high level, close to 1.0; Method 2 is volatile. When  $\Gamma = 0.2$ , Method 3 still performs well, and the accuracy of other methods fluctuates to varying degrees. The experimental data reflect the performance differences of different methods at different  $\Gamma$  values.

The left diagram in Fig. 10 shows the normalized load fluctuation curve within the typhoon impact period (8 days) under the three scenarios S1, S2 and S3. It can be seen that the load fluctuation range is significantly narrowed to  $\pm 0.15$  after S3 regulation, which verifies the effect of collaborative optimization on improving system stability. The scatter plot on the right presents the mapping relationship between unit load and utilization rate. The S2 scenario achieves a utilization rate of 0.85 at 150-unit load, an increase of 12% compared with S1, indicating that the agent collaborative strategy can effectively optimize resource scheduling efficiency and provide energy during typhoon. Provide technical support for balance between supply and demand.

Fig. 11 shows the changes in the power of each part of the comprehensive energy and the Total power (Total) at different

times when dealing with typhoon events. From the time span of 0-800 seconds, multiple power curves are intertwined. Taking P2-power and P1-power as examples, the power fluctuates significantly in some periods, such as around 500-600 seconds, each power component changes significantly, and the total power curve also fluctuates accordingly, reflecting the dynamic response characteristics of the integrated energy system under typhoon.

Fig. 12 shows the dynamic response characteristics of key performance indicators of multi energy flow system collaborative regulation during the iteration process in the typhoon disaster scenario. Combined with the functional positioning of five types of intelligent agents (S1-S5) in the typhoon "warning outbreak retreat" stage, the dynamic adaptability of their regulation mechanism can be analyzed. The upper left subgraph shows that during the warning stage (early stage of iteration), the peak regulation amount of S3 (emergency energy supply intelligent agent) reaches 38 units to ensure critical loads, while the regulation amount of S1-S2 (conventional energy dispatch intelligent agent) and S4-S5 (load side response intelligent agent) is relatively low; During the outbreak phase (mid iteration), S1-S2 enhances the regulation intensity, S4-S5 assists in load balancing, and the regulation volume of the three types of intelligent agents increases in synergy; In the fading stage (later stage of iteration), after three strategy adjustments (1  $\rightarrow$  2, 2  $\rightarrow$  3), all intelligent agents' control quantities converged, and S3 fell first; The MAE index (prediction error) in the upper right

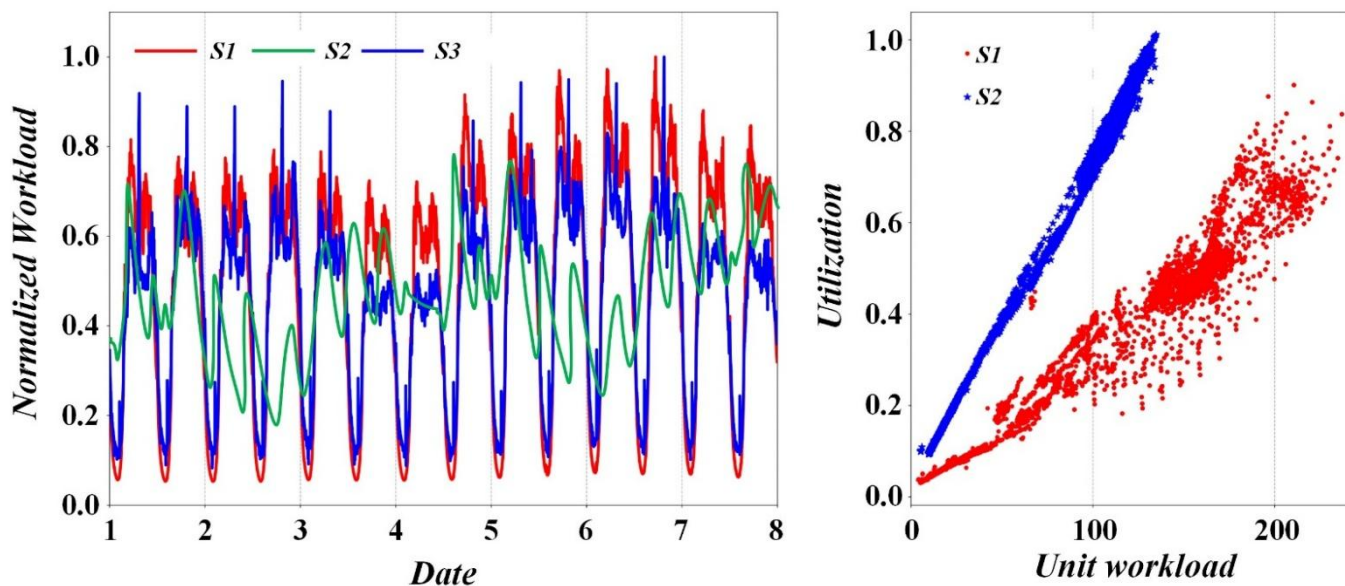


Fig. 10: Analysis of multi-agent regulation performance of integrated energy system during typhoon.

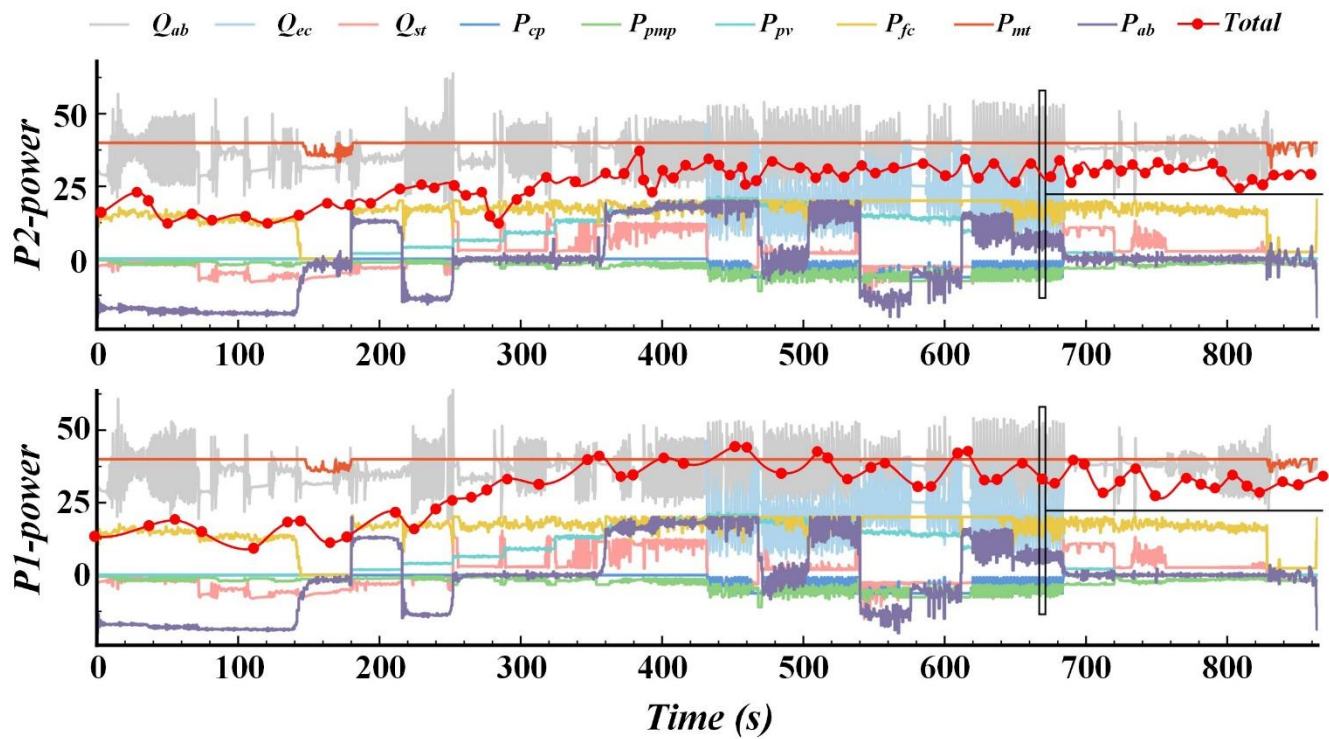


Fig. 11: Changes of comprehensive energy power in response to typhoon events.

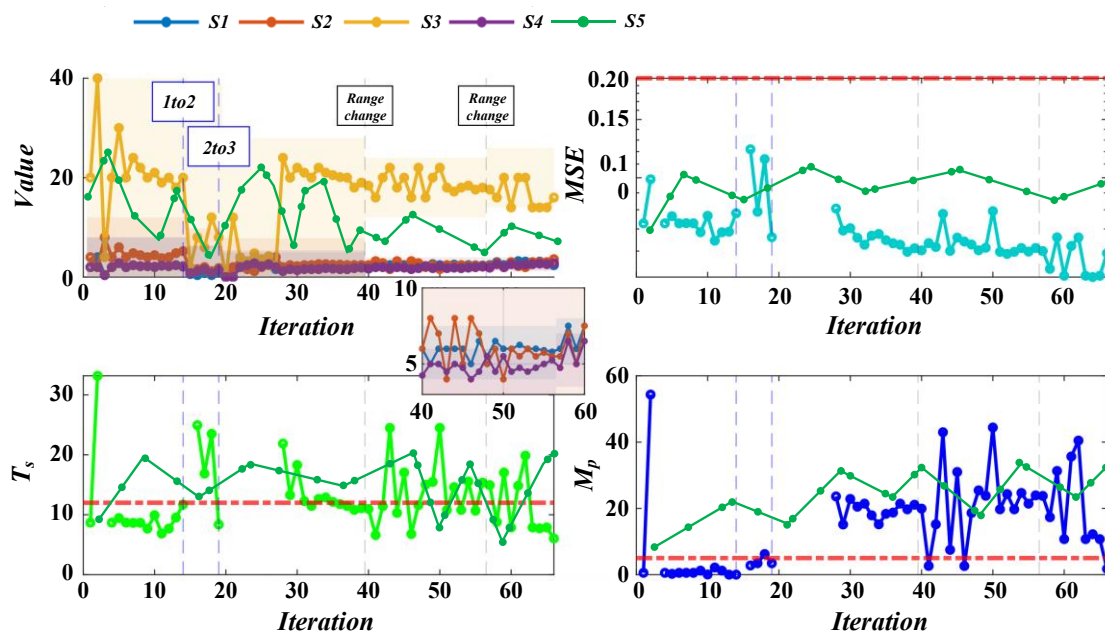


Fig. 12: Evolution analysis of collaborative optimization control performance of multi-agent system in response to typhoon events.

subgraph are mainly stable below 0.08 after 20 iterations, verifying the self optimization ability of prediction accuracy; In the lower left graph, the  $T_s$  index fluctuates during the initial iteration (5-15 times) due to energy supply interruptions, gradually approaching the expected threshold of 10 units; The  $M_p$  index (regulation stability) in the lower right graph showed a peak fluctuation of 23% during the middle of the iteration (30-40 times), but it quickly recovered without causing system instability; These data validate the

effectiveness of the proposed method, and the five types of intelligent agents can achieve differentiated coordination and convergence of control quantities through dynamic adjustment of functions. The system's key indicators perform well, proving its ability to quickly converge and dynamically balance in extreme disaster scenarios, providing a guarantee for the safe operation of multi energy flow systems during disasters.

## 5. Conclusion

In view of the impact of typhoon disasters on the integrated energy system, this study proposes a regulation method based on multi-agent collaborative optimization, which enables the dynamic balance and rapid recovery of the multi-energy flow system through a distributed decision-making framework. At the theoretical level, a hierarchical collaborative model comprising five types of agents, including interface agents and hazard factor agents, is constructed. Combined with weighted centrality and intermediary centrality indexes in social network analysis, an adaptive trigger mechanism that integrates typhoon warning levels is designed. In the method innovation, the alternating direction multiplier method is employed to decompose the global optimization problem, and robust optimization is introduced to address the uncertainty of typhoon parameters. The convergence of the algorithm is proved by Lyapunov-Krasovskii stability theory. Experimental verification demonstrates that this method significantly enhances system performance in extreme typhoon scenarios.

In the simulated line fault scenario, multi-agent cooperative regulation reduces the average voltage deviation of key nodes from 0.17 p.u. to 0.05 p.u., and the deviation optimization range of node 10 reaches 71.4%, which verifies the improvement effect of cooperative strategy on voltage stability.

In view of the 24-hour continuous typhoon scenario, coordinated regulation and control increased the system power supply reliability from 82.3% to 95.6% (an increase of 16.0%), and the renewable energy consumption rate increased by 20.7 percentage points to 89.2%. At the same time, the comprehensive operating cost was reduced by 21.1%, resulting in a savings of 2,630 yuan, which reflects the economic advantages of multi-energy complementarity.

Through iterative optimization analysis, it is found that the regulation amount of agent S3 converges from the peak value of 38 units to the steady state after three strategy adjustments, the system prediction error MAE stabilizes below 0.08 after 20 iterations, and the power fluctuation is controlled within 23% during 30-40 iterations, indicating that the algorithm has the ability of rapid response and dynamic balance.

Through theoretical modelling and experimental analysis, this study reveals the optimization potential of a multi-agent collaboration mechanism under typhoon disasters, providing key technical support for enhancing the resilience of integrated energy systems. Future research focus breakthrough direction: Building a dynamic perception model that integrates typhoon characteristics and multi energy flow laws to achieve accurate pre disaster prediction, innovating a multi-agent

layered collaborative framework to solve information synchronization and conflict problems, optimizing the multi-agent adaptive learning mechanism to improve real-time scheduling in extreme scenarios, establishing a "pre disaster mid disaster post disaster" full cycle optimization system, combining cross regional interconnection and energy storage collaboration, and balancing system resilience and cost-effectiveness through efficient algorithms.

## Acknowledgments

The work was financially supported by Science and Technology Projects from State Grid Corporation of China, (Research and demonstration of multi-agent collaboration and interaction technology for urban regional integrated energy system to strengthen grid resilience, No.:5400-202317577A-3-2-ZN).

## Conflict of Interest

All authors declare that they have no conflict of interest.

## Supporting Information

Not applicable.

## CRedit Statement

**Zhenlan Dou:** Original draft. **Chunyan Zhang:** Data collection. **Songcen Wang:** Formal analysis. **Yipan Zhang:** Validation. **Tao Zhang:** Data curation. **Dejian Yang:** Review & editing, Supervision. All authors read and approved the final manuscript.

## References

- [1] S. Gao, T. Yang, Y. Xu, N. Mou, X. Wang, H. Huang, Enhancing disaster situation awareness through multimodal social media data: evidence from typhoon Haikui, *Applied Sciences*, 2025, **15**, 465, doi: 10.3390/app15010465.
- [2] H. Hou, C. Liu, R. Wei, H. He, L. Wang, W. Li, Outage duration prediction under typhoon disaster with stacking ensemble learning, *Reliability Engineering & System Safety*, 2023, **237**, 109398, doi: 10.1016/j.ress.2023.109398.
- [3] D. K. Asl, A. R. Seifi, M. Rastegar, M. Dabbaghjamanesh, N. D. Hatziaargyriou, Distributed two-level energy scheduling of networked regional integrated energy systems, *IEEE Systems Journal*, 2022, **16**, 5433-5444, doi: 10.1109/JSYST.2022.3166845.
- [4] Z. Dong, K. Hou, Z. Liu, X. Yu, H. Jia, Q. Xiao, A deep-learning-based optimal energy flow method for reliability assessment of integrated energy systems, *IEEE Access*, 2022, **10**, 91092-91102.
- [5] A. Farzamnia, S. Marjani, S. Galvani, K. T. T. Kin, Optimal allocation of soft open point devices in renewable energy integrated distribution systems, *IEEE Access*, 2022, **10**, 9309-9320.
- [6] H. Cheng, Q. Ai, Federated learning application in distributed

- energy trading in integrated energy system, *Energy Reports*, 2023, **10**, 484-493, doi: 10.1016/j.egy.2023.06.040.
- [7] Z. Ding, H. Qing, K. Zhou, J. Huang, C. Liang, L. Liang, N. Qin, L. Li, Integrated energy system load forecasting with spatially transferable loads, *Energies*, 2024, **17**, 4843, doi: 10.3390/en17194843.
- [8] G. Chen, Z. Ming, J. Milisavljevic-Syed, H. Xia, K. Salonitis, G. Wang, Y. Yan, Shared mental models-based collaboration method in assembly tasks for multi-agent self-organizing systems, *Advanced Engineering Informatics*, 2025, **66**, 103494, doi: 10.1016/j.aei.2025.103494.
- [9] J. Gao, Z. Shao, F. Chen, M. Lak, Robust optimization for integrated energy systems based on multi-energy trading, *Energy*, 2024, **308**, 132302, doi: 10.1016/j.energy.2024.132302.
- [10] S. Chen, L. Rui, Z. Gao, Y. Yang, X. Qiu, S. Guo, Service migration with edge collaboration: multi-agent deep reinforcement learning approach combined with user preference adaptation, *Future Generation Computer Systems*, 2025, **165**, 107612, doi: 10.1016/j.future.2024.107612.
- [11] H. Gao, R. Wang, S. He, L. Wang, J. Liu, Z. Chen, A cloud-edge collaboration solution for distribution network reconfiguration using multi-agent deep reinforcement learning, *IEEE Transactions on Power Systems*, 2024, **39**, 3867-3879, doi: 10.1109/TPWRS.2023.3296463.
- [12] J. Gao, W. Zhang, T. Guan, Q. Feng, Evolutionary game study on multi-agent collaboration of digital transformation in service-oriented manufacturing value chain, *Electronic Commerce Research*, 2023, **23**, 2217-2238, doi: 10.1007/s10660-022-09532-0.
- [13] H. Hou, J. Tang, Z. Zhang, Z. Wang, R. Wei, L. Wang, H. He, X. Wu, Resilience enhancement of distribution network under typhoon disaster based on two-stage stochastic programming, *Applied Energy*, 2023, **338**, 120892, doi: 10.1016/j.apenergy.2023.120892.
- [14] H. Hou, Z. Zhang, J. Yu, R. Wei, Y. Huang, X. Li, Damage prediction of 10 kV power towers in distribution network under typhoon disaster based on data-driven model, *International Journal of Electrical Power & Energy Systems*, 2022, **142**, 108307, doi: 10.1016/j.ijepes.2022.108307.
- [15] X. Gong, T. Wang, T. Huang, Y. Cui, Toward safe and efficient human-swarm collaboration: a hierarchical multi-agent pickup and delivery framework, *IEEE Transactions on Intelligent Vehicles*, 2023, **8**, 1664-1675, doi: 10.1109/TIV.2022.3172342.
- [16] X. Guo, D. Shi, J. Yu, W. Fan, Heterogeneous multi-agent reinforcement learning for zero-shot scalable collaboration, *Neurocomputing*, 2025, **648**, 130716, doi: 10.1016/j.neucom.2025.130716.
- [17] X. Liu, S. Xie, J. Tian, P. Wang, Two-stage scheduling strategy for integrated energy systems considering renewable energy consumption, *IEEE Access*, 2022, **10**, 83336-83349.
- [18] P. Gao, Y. Yang, F. Li, J. Ge, Q. Yin, R. Wang, Research on integrated decision making of multiple load combination forecasting for integrated energy system, *Energy*, 2024, **311**, 133390, doi: 10.1016/j.energy.2024.133390.
- [19] S. M. Ghania, Risk analysis of energy systems integrated with renewable energy resources, *IEEE Access*, 2024, **12**, 25590-25597.
- [20] A. Guan, S. Zhou, W. Gu, J. Chen, H. Lv, Y. Fang, J. Xv, Enhancing stability of electric-steam integrated energy systems by integrating steam accumulator, *Applied Energy*, 2024, **364**, 123049, doi: 10.1016/j.apenergy.2024.123049.
- [21] K. Huang, M. Fu, X. Ding, Security and economic integration scheduling of electricity-heat integrated energy system, *IEEE Access*, 2023, **11**, 112236-112247.
- [22] H. Guo, H. Yu, M. Wang, C. Liu, C. Li, Integrated management of workloads and energy system for data centers, *Energy*, 2025, **327**, 136400, doi: 10.1016/j.energy.2025.136400.
- [23] Y. Hu, B. Yang, P. Wu, X. Wang, J. Li, Y. Huang, R. Su, G. He, J. Yang, S. Su, J. Wang, L. Jiang, Y. Sang, Optimal planning of electric-heating integrated energy system in low-carbon park with energy storage system, *Journal of Energy Storage*, 2024, **99**, 113327, doi: 10.1016/j.est.2024.113327.
- [24] S. Huang, H. Lu, M. Chen, W. Zhao, Integrated energy system scheduling considering the correlation of uncertainties, *Energy*, 2023, **283**, 129011, doi: 10.1016/j.energy.2023.129011.
- [25] W. Jiang, R. Qi, S. Xu, S. Hashimoto, Real-time simulation system for small scale regional integrated energy systems, *Energies*, 2024, **17**, 3211, doi: 10.3390/en17133211.
- [26] S. Li, Y. Lin, H. Huang, Relief supply-demand estimation based on social media in typhoon disasters using deep learning and a spatial information diffusion model, *ISPRS International Journal of Geo-Information*, 2024, **13**, 29, doi: 10.3390/ijgi13010029.
- [27] S. Li, Y. Wang, H. Huang, L. Huang, Y. Chen, Study on typhoon disaster assessment by mining data from social media based on artificial neural network, *Natural Hazards*, 2023, **116**, 2069-2089, doi: 10.1007/s11069-022-05754-5.
- [28] F. Liu, E. Xu, H. Zhang, An improved typhoon risk model coupled with mitigation capacity and its relationship to disaster losses, *Journal of Cleaner Production*, 2022, **357**, 131913, doi: 10.1016/j.jclepro.2022.131913.
- [29] G. Liu, J. Yin, S. Song, W. Yang, Y. Tian, L. Wang, Y. Xu, Risk estimation of typhoon disaster based on three-dimensional information diffusion method, *Journal of Marine Science and Engineering*, 2023, **11**, 1080, doi: 10.3390/jmse11051080.
- [30] Y. Lu, S. Qiao, Y. Yao, Risk assessment of typhoon disaster chain based on knowledge graph and Bayesian network, *Sustainability*, 2025, **17**, 331, doi: 10.3390/su17010331.
- [31] J. Huang, H. Zhang, D. Tian, Z. Zhang, C. Yu, G. P. Hancke, Multi-agent deep reinforcement learning with enhanced collaboration for distribution network voltage control, *Engineering Applications of Artificial Intelligence*, 2024, **134**, 108677, doi: 10.1016/j.engappai.2024.108677.
- [32] F. Si, N. Zhang, Y. Wang, P.-Y. Kong, W. Qiao, Distributed optimization for integrated energy systems with secure multiparty computation, *IEEE Internet of Things Journal*, 2023, **10**, 7655-7666, doi: 10.1109/JIOT.2022.3209017.
- [33] M. M. Karim, D. H. Van, S. Khan, Q. Qu, Y. Kholodov, AI agents meet blockchain: a survey on secure and scalable collaboration for multi-agents, *Future Internet*, 2025, **17**, 57, doi:

10.3390/fi17020057.

[34] F. Li, X. Li, S. Wen, H. Huang, J. Bao, SAMAC-R3-MED: semantic alignment and multi-agent collaboration of retriever-reranker-responder models for multimodal engineering documents, *Computers in Industry*, 2025, **171**, 104336, doi: 10.1016/j.compind.2025.104336.

[35] J. Li, F. Wu, H. Shi, K.-S. Hwang, A collaboration of multi-agent model using an interactive interface, *Information Sciences*, 2022, **611**, 349-363, doi: 10.1016/j.ins.2022.07.052.

**Publisher's Note:** Engineered Science Publisher remains neutral with regard to jurisdictional claims in published maps and institutional affiliations.

### Open Access

This article is licensed under a Creative Commons Attribution 4.0 International License, which permits the use, sharing, adaptation, distribution and reproduction in any medium or format, as long as appropriate credit to the original author(s) and the source is given by providing a link to the Creative Commons license and changes need to be indicated if there are any. The images or other third-party material in this article are included in the article's Creative Commons license, unless indicated otherwise in a credit line to the material. If material is not included in the article's Creative Commons license and your intended use is not permitted by statutory regulation or exceeds the permitted use, you will need to obtain permission directly from the copyright holder. To view a copy of this license, visit <http://creativecommons.org/licenses/by/4.0/>.

©The Author(s) 2025.